MAGNETIC RESONANCE IN CHEMISTRY
Magn. Reson. Chem. 2004; **42**: 267–275
Published online in Wiley InterScience (www.interscience.wiley.com). DOI: 10.1002/mrc.1330

MRC

Investigation of the dynamics of an elastin-mimetic polypeptide using solid-state NMR

Xiao L. Yao,[1] Vincent P. Conticello[2] and Mei Hong[1]*

[1] Department of Chemistry, Iowa State University, Ames, Iowa 50011, USA
[2] Department of Chemistry, Emory University, Atlanta, Georgia 30322, USA

Received 18 February 2003; Revised 14 June 2003; Accepted 25 June 2003

Elastin is the main structural protein that provides elasticity to various tissues and organs in vertebrates. Molecular motions are believed to play a significant role in its elasticity. We have used solid-state NMR spectroscopy to characterize the dynamics of an elastin-mimetic protein as a function of hydration to better understand the origin of elastin elasticity. Poly(Lys-25), $[(VPGVG)_4(VPGKG)]_{39}$, has a repeat sequence common to natural elastin. ^{13}C cross-polarization and direct polarization spectra at various hydration levels indicate that water enhances the protein motion in a non-uniform manner. Below 20% hydration, the backbone motion increases only slightly whereas above 30% hydration, both the backbone and the side-chains undergo large-amplitude motions. The motional amplitudes are extracted from ^{13}C–^{1}H and ^{1}H–^{1}H dipolar couplings using 2D isotropic–anisotropic correlation experiments. The root mean square fluctuation angles are found to be 11–18° in the dry protein and 16–21° in the 20% hydrated protein. Dramatically, the amplitudes increase to near isotropic at 30% hydration. Field-dependent ^{1}H rotating-frame spin–lattice relaxation times ($T_{1\rho}$) indicate that significant motions occur on the microsecond time-scale (1.2–2.3 μs). The large-amplitude and low-frequency motion of poly(Lys-25) at relatively mild hydration indicates that the conformational entropy of the protein in the relaxed state contributes significantly to the elasticity.

KEYWORDS: solid-state NMR; elastin; dynamics; relaxation time; motional averaging; dipolar coupling

INTRODUCTION

Elastin is an extracellular matrix protein that is responsible for the elasticity of lungs, arteries and skins. Elastin contains two domains: the hydrophobic domain mainly consists of residues such as Ala, Gly, Val and Leu, whereas the hydrophilic domain, rich in Lys and Ala, cross-links the hydrophobic segments, thus forming the elastic fibers. Elastin elasticity is entropic in origin; however, whether this entropy mainly derives from the conformational motion of the polypeptide chains or from hydrophobic hydration is not clearly understood. In the librational elasticity model, proposed by Urry and co-workers based on studies of $(VPGVG)_n$ proteins, residues between adjacent Pro–Gly moieties undergo large-amplitude and low-frequency librational motions in the relaxed state. Upon extension, these motions decrease in amplitude and increase in frequency, thus decreasing the entropy of the system and providing the elastomeric restoring force[1]. Dabelle and Tamburro studied the GXGGX repeat sequences and attributed the entropy change to a transition from chaotic conformational interconversions between labile β-turns in the relaxed state to non-linear vibrational motions in the stretched state.[2] In contrast to these conformational entropy models, the 'oiled coil' model[3] and the 'liquid drop' model[4] postulate that the entropic elasticity originates from the reduction of the configurational entropy of the protein–water two-phase system when hydrophobic side-chains are exposed to water upon extension.[5] Water is known to play an extremely important role in elastin function, since only water-swollen elastin exhibits elasticity.[6,7] Therefore, to elucidate the molecular basis for elastin elasticity, it is crucial to examine the interaction between the protein and the water.

Solid-state NMR spectroscopy is a powerful tool for studying molecular motions in proteins. It has been used to reveal the functional importance of protein motions in a number of structural polypeptides. For example, in collagen fibrils, ^{2}H and ^{13}C NMR showed that side-chains undergo large-amplitude reorientational motions around the triple helix axis whereas the backbone is relatively rigid.[8–10] This combination imparts high tensile strength to the protein while allowing stress to be absorbed uniformly. ^{13}C and ^{2}H NMR showed that the supercontraction of dragline spider silk upon wetting is directly correlated with the onset of large-amplitude motions.[11] Fleming *et al*. examined ^{13}C spin–lattice relaxation times (T_1) and linewidths of carbonyl-labeled chick aortic elastin and found the hydrophobic region to be highly mobile. Moreover, the mobility is strongly influenced by protein–solvent interactions and temperature.[12] Perry *et al*. recently carried out a systematic

*Correspondence to: Mei Hong, Department of Chemistry, Iowa State University, Ames, Iowa 50011, USA.
E-mail: mhong@iastate.edu
Contract/grant sponsor: Iowa State University.

study of this temperature and hydration dependence of the dynamics of bovine nuchal elastin, and confirmed that fully hydrated elastin exhibits a substantial increase of mobility compared with the dry or the frozen protein.[13]

The present study was aimed at obtaining more quantitative information on the amplitudes and rates of hydration-induced motions in elastin. We used both 1D and 2D solid-state NMR techniques to characterize the detailed dynamics of an elastin-mimetic polypeptide. The recombinant protein has an amino acid sequence $[(VPGVG)_4(VPGKG)]_{39}$ (81 kDa) and is designated poly(Lys-25).[14] The VPGVG motif is one of the most common repeat sequences in natural elastin. Urry *et al*. have shown that VPGVG polypeptides exhibit similar mechanical properties to elastin.[15–17] Specifically, poly(Lys-25) exhibits an inverse temperature transition to a gel state and displays a beaded filamentous network morphology characteristic of natural elastin under electron microscopes.[14] The recombinant protein is easy to produce in large quantities and can be readily labeled with ^{13}C and ^{15}N, thus facilitating solid-state NMR studies. These properties make poly(Lys-25) an excellent model system for studying elastin hydration dynamics. In this work, we compared ^{13}C cross-polarization (CP) and direct polarization (DP) spectra under various hydration levels to characterize motional heterogeneity in poly(Lys-25). We then measured the ^1H–^1H and ^{13}C–^1H dipolar couplings in a site-resolved manner to determine the amplitudes of segmental motions as a function of hydration. Slow motions on the microsecond time-scale were further probed from ^1H $T_{1\rho}$ relaxation times. These experiments indicate that water induces segmental motions in poly(Lys-25) in a non-uniform manner. Moreover, at ca 30% hydration, poly(Lys-25) undergoes much larger amplitude motions than most other solid proteins.

EXPERIMENTAL

Poly(Lys-25) has an amino acid sequence $[(VPGVG)_4(VPGKG)]_{39}$ and a molecular weight of 81 kDa. It was cloned and expressed in M9 medium as described previously.[14] About 40 mg of unlabeled poly(Lys-25) was packed into a 4 mm magic angle spinning (MAS) rotor. The sample was hydrated by direct addition of deionized water to the lyophilized protein and equilibrated for an extended period of time before the NMR experiments. To achieve homogeneous hydration, water was added incrementally to small amounts of sample until the desired hydration level. Well hydrated samples appear light yellow and have the consistency of gels. The water content is expressed as weight percentage of the total sample mass. For the 20% hydrated sample, a ^{13}C,^{15}N-labeled protein was used. The ^{13}C-labeled sites are Val Cα and Cβ, Gly Cα, Pro Cα, Cβ, Cδ, and CO, and Lys Cα, Cγ, Cδ and Cε. This leaves unlabeled carbons at Pro Cγ, Val Cγ, Lys Cβ and CO and the carbonyl carbon of Val and Gly. The selectivity of ^{13}C labeling was achieved by using [2-^{13}C]glycerol as the sole carbon precursor in the expression media and was verified by the lack of the Pro Cγ signal and the weakness of the Val Cγ signal in the ^{13}C spectra.[18] This selective and extensive ^{13}C labeling protocol both enhances the spectral sensitivity and preserves spectral resolution compared with uniformly ^{13}C-labeled proteins. It has been demonstrated on a number of proteins such as ubiquitin,[19] colicin Ia channel domain[20] and α-spectrin SH3 domain.[21,22]

NMR spectra were collected on a DSX-400 spectrometer (Bruker, Karlsruhe, Germany) operating at a magnetic field of 9.4 T, which corresponds to a ^{13}C resonance frequency of 100.72 MHz. A triple-resonance MAS probe equipped with a 4 mm spinning module was used. Typical radio frequency (r.f.) field strengths for the ^1H channel were 85 kHz for decoupling and 50 kHz for CP. The carbon 90° pulse length was typically 4–5 μs. All experiments were conducted at 293 ± 2 K.

We used 2D wide-line separation (WISE)[23] experiments to measure ^1H–^1H dipolar couplings. After a ^1H 90° pulse, the ^1H magnetization evolves under the combination of ^1H–^1H and ^1H–^{13}C dipolar couplings, and is then transferred to ^{13}C via a short (100–200 μs) Lee–Goldburg (LG) CP[24,25] period. LG–CP instead of Hartman–Hahn CP was used in order to obtain site-specific dipolar couplings. The experiments were performed at a spinning speed $\omega_r/2\pi$ of 4 kHz. The maximum evolution time t_1 is 0.7 ms for the dry protein and 1 ms for the wet samples.

^{13}C–^1H dipolar couplings between directly bonded C–H spins were measured using the 2D LG–CP experiment.[26,27] The evolution time (t_1) of the experiment is the CP contact time. In the spin space, the ^1H magnetization is locked along the magic angle direction relative to the static magnetic field to prevent ^1H spin diffusion. Thus, at short contact times (<1 ms), mostly directly bonded ^{13}C–^1H dipolar couplings are observed. ^{13}C detection during t_2 resolves the ^{13}C–^1H couplings according to the ^{13}C isotropic chemical shifts. The spinning speeds for the LG–CP experiments were 8–12 kHz and the maximum t_1 was 2 ms. The relatively high spinning speed was used to achieve efficient polarization transfer at the first sideband condition, $\omega_{1C} = \omega_{eff,H} - \omega_r$, where ω_{1C} is the ^{13}C spin lock field strength and $\omega_{eff,H}$ is the effective spin lock field strength of ^1H.[27] For the 30% hydrated protein, the ^1H $T_{1\rho}$ decreases significantly, which interferes with the measurement of small C–H dipolar couplings. To minimize the effects of short ^1H $T_{1\rho}$, a variable ^1H LG spin lock period was inserted before LG–CP, such that the sum of the spin lock and CP periods is constant [see Fig. 4(d)].

The ^1H rotating-frame spin–lattice relaxation times ($T_{1\rho}$) were measured using a ^1H LG spin lock period before LG–CP to ^{13}C. By using magic-angle spin lock throughout the sequence on the ^1H spins, we suppress ^1H spin diffusion, so that the $T_{1\rho}$ of ^1H spins directly bonded to the detected ^{13}C site is measured. Two ^1H spin-lock field strengths, 50 and 75 kHz, were used. The ratio of the two $T_{1\rho}$ values yields information on the motional correlation times without requiring knowledge of the exact order parameters.[25]

All ^{13}C chemical shifts were referenced to TMS indirectly through the Gly carbonyl signal (176.4 ppm).

RESULTS

Hydration-dependent ^{13}C CP and DP spectra

Figure 1 shows the 1D ^{13}C CP and DP spectra of poly(Lys-25) with varying water contents. Peak assignment was obtained

from 2D correlation experiments presented elsewhere.[18] Comparisons of the CP and DP spectra provide valuable information on motional heterogeneity. Rigid segments exhibit high intensities in the CP spectra, since strong $^{13}C-^{1}H$ dipolar couplings are required for efficient polarization transfer. On the other hand, mobile groups are preferentially enhanced in the DP spectra owing to their motionally narrowed linewidths and their short ^{13}C spin–lattice relaxation times. Figure 1 shows that higher water content reduces the CP intensities while increasing the DP intensities, indicating that hydration increases segmental motions. The motion is heterogeneous. At low hydration levels (<20%), assuming similar CP efficiencies, the relative intensities of the side-chains (10–40 ppm) to backbone Cα (40–70 ppm) are lower than dictated by their relative abundance in the protein. This indicates that the side-chains are more mobile than the backbone. With increasing water, the Cα intensities increase in the DP spectra but decrease in the CP spectra, indicating increased motion in the protein backbone. At 30% hydration, the ratio of the integrated intensities for the backbone and the side-chains in the CP spectrum is about 1 : 1.3, which match the relative abundance of these two groups in poly(Lys-25). While the intensity estimate is only semi-quantitative, it nevertheless suggests that relative to other water levels, 30% is the stage where the protein mobility is relatively uniform throughout the molecule. While the backbone mobility is primarily induced by hydration, the side-chain motion results from both the chain conformational flexibility and hydration. Further addition of water to 40% reduced the methyl signals dramatically while broadening the Cα signals in the CP spectra. The former signifies the presence of near isotropic amplitude motion in the side-chains, while the latter suggests that motions on an intermediate time-scale comparable to the inverse of the ^{1}H decoupling field strength have increased in the backbone.[28]

A second observation from these 1D spectral series is that the protein dynamics increase with hydration in a non-uniform fashion. Between 0 and 20% water levels, both the CP and DP spectra changed little. However, at 30% hydration, the backbone CP signals decreased twofold. Meanwhile, the linewidths of the resolved side-chain signals in the DP spectra decreased by a factor of 2–2.5; for example, the Val methyl signal narrowed from 310 to 150 Hz. Therefore, large-amplitude motions begin at about 20–30% hydration in poly(Lys-25). This is in excellent agreement with the non-uniform hydration dependence seen in bovine nuchal ligament elastin, where two distinct hydration regimes, below and above the ca 25% water level,[13] can be clearly distinguished.

The Lys residue occurs rarely (one in every 25 residues) in poly(Lys-25), hence its ^{13}C signals is unobservable at low hydration. However, as the water level increases above 20%, the well labeled Lys Cε (40 ppm) and Cγ (27 ppm) sites[19] become detectable in the DP spectra. Hence the hydrophilic side-chains of Lys are highly mobile at high water contents and are probably in close contact with the water molecules.

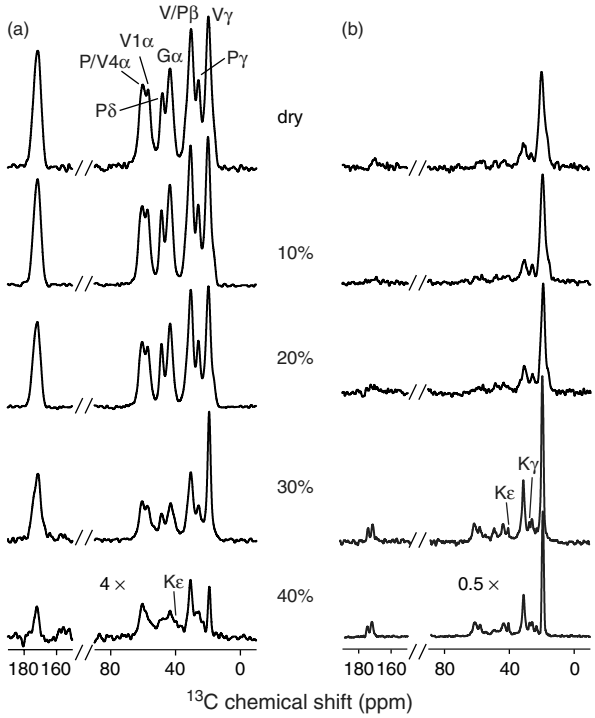

Figure 1. ^{13}C spectra of poly(Lys-25) at various hydration levels. (a) CP spectra; (b) DP spectra. Assignment is indicated based on the characteristic chemical shifts of amino acids and 2D correlation experiments performed on ^{13}C,^{15}N-labeled poly(Lys-25).[18].

$^{1}H-^{1}H$ and $^{13}C-^{1}H$ dipolar couplings in poly(Lys-25)

To obtain more quantitative information on the motional amplitudes of poly(Lys-25) as a function of water level, we measured $^{1}H-^{1}H$ and $^{1}H-^{13}C$ dipolar couplings using the 2D LG–WISE and 2D LG–CP experiments. Rigid segments exhibit strong dipolar couplings and thus large splittings in the LG–CP spectra and broad lines in the WISE spectra, while mobile groups show reduced coupling strengths. The ^{13}C isotropic chemical shift dimension provides site resolution to the 2D spectra.

Representative 2D WISE spectra [Fig. 2(a) and (b)] and several dipolar cross-sections [Fig. 2(c)–(f)] are shown. The

Table 1. $^{1}H-^{1}H$ dipolar couplings (kHz) of poly(Lys-25) at three hydration levels

Residue	Dry	20% H_2O	30% H_2O
P/V4α	57.8	56.2	12.5
V1α	59.4	59.4	12.5
Gα	67.2	65.6	29, 7.8
Pδ	67.2	67.2	NA[a]
V/Pβ	57.8	50.0	12.5
Pγ	57.8	NA[a]	12.5
Vγ	28.1	23.4	12.5

[a] The signals are not observed owing to either lack of labeling or motional attenuation.

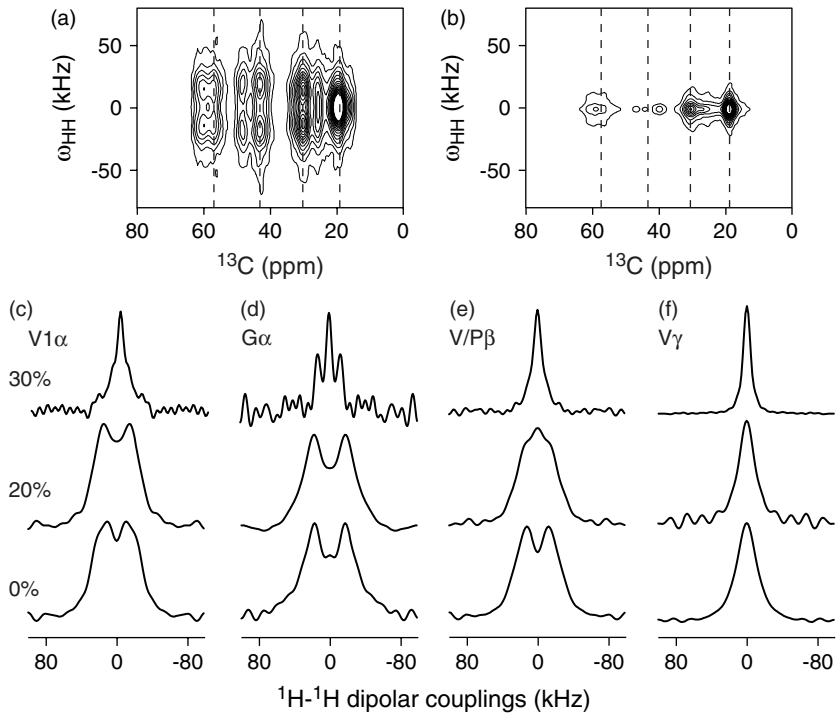

Figure 2. 2D LG–WISE spectra of poly(Lys-25) at various hydration levels. The 2D spectra for the dry (a) and 30% hydrated (b) protein show the substantial loss of intensity for the backbone sites in the hydrated protein. Several ^{1}H cross-sections are extracted: (c) Val-1 Cα; (d) Gly Cα; (e) Val/Pro Cβ; (f) Val Cγ. The dry, 20% hydrated and 30% hydrated spectra are arranged from bottom to top.

full widths at half-maximum (FWHM) of these WISE patterns, listed in Table 1, provide semi-quantitative information on the degree of motional narrowing. In the dry protein, the FWHMs are about 59 kHz for CH groups, 67 kHz for CH_2 groups and 28 kHz for CH_3 groups. Increasing the water level to 20% did not change the backbone coupling significantly (weaker by ca 5%), as shown for Val-1 Cα [Fig. 2(c)] and Gly Cα [Fig. 2(d)], but reduced the side-chain couplings more ($\sim$15%), as shown for Val/Pro Cβ [Fig. 2(e)] and Val Cγ [Fig. 2(f)]. The unlabeled Pro Cγ also gives a clearly reduced ^{1}H–^{1}H dipolar coupling (data not shown). Contrary to the limited differences between the 0% and the 20% samples, a drastic line narrowing was detected in the 30% hydrated protein, with the FWHM for most sites reduced to about 12.5 kHz. The spectral sensitivity and resolution also deteriorated, especially for Pro Cδ and Gly Cα [Fig. 2(d)], owing to inefficient CP. Closer inspection indicates that some sites (e.g. Gly Cα) not only have a high-intensity narrow component but also a broader component, suggesting inhomogeneous dynamics in the protein. For the narrow component, the couplings of the backbone and the side-chains are more similar than in the dry protein. This is consistent with the observation from the 1D spectra that hydration to 30% achieves comparable mobility in the protein backbone and the side-chains.

Compared with the ^{1}H WISE spectra, ^{13}C–^{1}H dipolar couplings provide more quantitative values of the motional amplitudes. For a rigid segment, the C–H dipolar splitting observed in an LG–CP spectrum is scaled from the one-bond ^{13}C–^{1}H coupling by a factor of cos(54.7°), yielding a rigid-limit C–H coupling of 13.3 kHz. Motionally induced line narrowing is represented by a bond order parameter, S_{CH}, which is the scaling factor between the measured coupling and the rigid-limit value. In practice, owing to vibrational averaging of the C—H bond[29,30] and experimental imperfections, the rigid-limit coupling for CH groups is slightly smaller, found to be 12.6 kHz based on model compound measurements.[27] The methylene groups exhibit a more complex LG–CP lineshape[31] and a rigid-limit splitting of 13.2 kHz.[27] Assuming the motion to be axially symmetric and sufficiently small in amplitude, the bond order parameters for CH groups can be converted to the root mean square (r.m.s.) angle of motion according to $S_{CH} = 1 - 3/2\langle\theta^2\rangle$.[32]

Figure 3 shows representative LG–CP dipolar cross-sections for Val-1 Cα, Gly Cα, Val/Pro Cβ and Val Cγ at 0, 20 and 30% hydration. In addition to the expected doublet splittings, zero-frequency intensities are observed in a number of cross-sections, which result from both long-range C–H dipolar couplings and mobile components in the sample. The experimental ^{13}C–^{1}H dipolar couplings and the motional scaling factors are summarized in Table 2. The protein is not completely rigid in the dry state, with an average order parameter S_{CH} of 0.94 for the backbone and Pro Cδ. The side-chains have slightly smaller order parameters of 0.7–0.8. These correspond to r.m.s. angles of 11–14° for the backbone and ca 20° for the side-chains. Consistent with the CP/DP results and the WISE spectra, hydration at or below 20% only mildly affects the protein. For example, for Val/Pro Cα, water reduced the C–H order parameters from 0.93 to 0.88 and increased the r.m.s. angle from 14 to 16°. Somewhat larger coupling reductions were detected for Gly Cα and Pro Cδ.

At 30% hydration, the overall intensities of the LG–CP spectra decreased dramatically owing to the onset of large-amplitude motions. More importantly, the ^{1}H $T_{1\rho}$

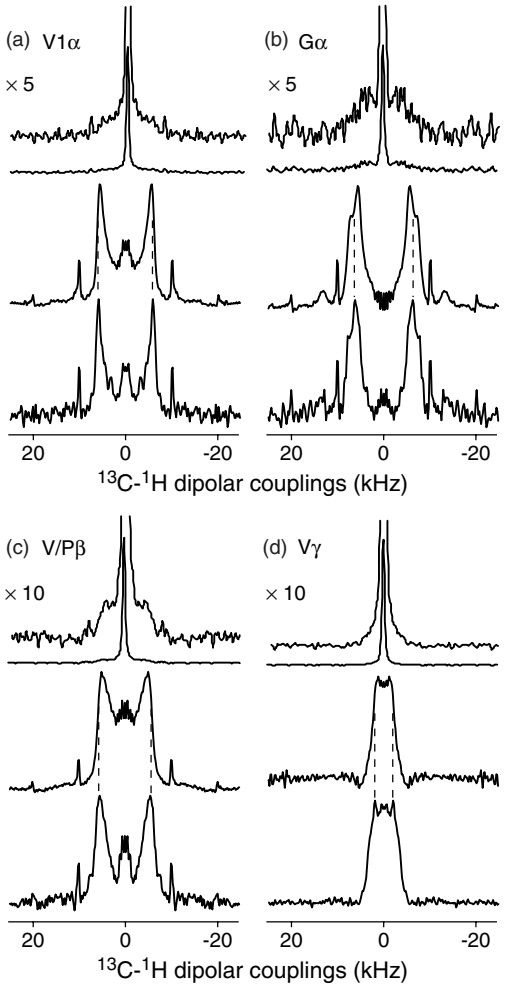

Figure 3. $^{13}C-^{1}H$ dipolar cross-sections of 2D LG–CP spectra of the dry (bottom), 20% hydrated (middle) and 30% hydrated (top) poly(Lys-25). (a) Val-1 Cα; (b) Gly Cα; (c) Val/Pro Cβ; (d) Val Cγ. The 30% hydration spectra are amplified to show the low intensities of the broad component.

Table 2. LG–CP $^{13}C-^{1}H$ dipolar splittings (δ_{CH}, kHz) and the corresponding motional scaling factor (S_{CH}) of poly(Lys-25) at three hydration levels

	Dry		20% H_2O		30% H_2O	
Residue	δ_{CH}	S_{CH}	δ_{CH}	S_{CH}	δ_{CH}[a]	S_{CH}
P/V4α	11.7	0.93	11.3	0.88	0.6	0.05
V1α	11.7	0.93	11.3	0.88	0.6	0.05
Gα	12.5	0.95	11.1	0.84	0.6	0.05
Pδ	12.5	0.95	10.7	0.81	NA[b]	NA[b]
V/Pβ	10.9	0.85	10.2	0.80	0.6	0.05
Pγ	9.4	0.71	NA[b]	NA[b]	0.6	0.05

[a] No C–H splitting is observed at 30% hydration (see Fig. 3), hence the couplings are measured as the FWHM of the lineshapes.

[b] The signals are not observed owing to either lack of labeling or motional attenuation.

relaxation time decreased significantly (see below), causing severe intensity loss within 0.8 ms. This interferes with the measurement of small couplings, which require CP contact times of at least 1.5 ms and preferably longer. Figure 4 shows that when the Val-1 Cα time signal is acquired using the normal LG–CP sequence, it exhibits a substantial $T_{1\rho}$ decay in <1 ms. To overcome this problem, we added a ^{1}H spin-lock period before the CP contact time to make the total ^{1}H spin-lock time constant [Fig. 4(d)]. This constant-time LG–CP technique removes the $T_{1\rho}$ effect in the time oscillations. The same Val-1 Cα signal now exhibits a slow rise [Fig. 4(b)] indicative of weak C–H dipolar couplings. Even at a maximum C–H evolution time of 1.6 ms, the rise is not yet complete. However, longer CP contact times become prohibitive owing to exponentially decreasing sensitivity. This contrasts dramatically with the Val-1 time signal in the dry protein [Fig. 4(e)], which shows fast initial oscillations and a constant plateau even after 2 ms of CP contact.

The Fourier-transformed C–H dipolar cross-sections for the constant-time LG–CP experiment for the 30% hydrated poly(Lys-25) are shown in the top row of Fig. 3. The dramatic line narrowing due to hydration is evident. Most sites exhibit no detectable splittings; using FWHM as the criterion, we find couplings of about 0.6 kHz, which is consistent with the rise constant in the time signal. Closer inspection indicates that this near isotropic component co-exists with a larger dipolar coupling of ca 4–8 kHz. This more rigid component manifests as the initial fast decay in the time signal, or the larger C–H coupling in the baseline of the frequency spectrum, and constitutes 20–40% of the total sample.

The dynamics of Pro Cγ are distinct from all other resolved sites in the protein. Even in the dry state it exhibits a much weaker C–H dipolar coupling compared with Pro Cδ, which is closer to the backbone. Increased hydration to 20 and 30% further reduced the C–H coupling. These indicate that Pro Cγ is the least restricted site among all methylene groups on the pyrrolidine ring. This additional flexibility may originate from two-site jumps due to ring puckering, which was previously observed in Pro-containing peptides in both solution and solid states.[33]

^{1}H $T_{1\rho}$ relaxation times

While the C–H and H–H dipolar couplings provide information on the amplitudes of motions, nuclear spin relaxation times reveal the rates of these motions. We measured the ^{1}H rotating-frame spin–lattice relaxation times ($T_{1\rho}$) in poly(Lys-25) to gain insight into relatively slow, microsecond time-scale, motions in the protein. The experiment utilizes a ^{1}H LG spin lock followed by LG–CP to ^{13}C, again to suppress ^{1}H spin diffusion and provide site-specific ^{1}H relaxation times. The $T_{1\rho}$ times were measured at two ^{1}H spin-lock field strengths, 50 and 75 kHz, to facilitate the extraction of the motional correlation times (see below). Figure 5 shows the representative $T_{1\rho}$ curves of Val-1 Cα at the three water levels. The ^{1}H $T_{1\rho}$ decreases both with increasing hydration and with decreasing spin lock field strength. The decrease is small between 0 and 20% water levels, but substantial from 20 to 30% hydration, with final $T_{1\rho}$ values of <1 ms for most sites compared with the initial value of about 15 ms in the dry protein.

The B_1-field dependence of ^{1}H $T_{1\rho}$ relaxation times permits the determination of motional correlation times,

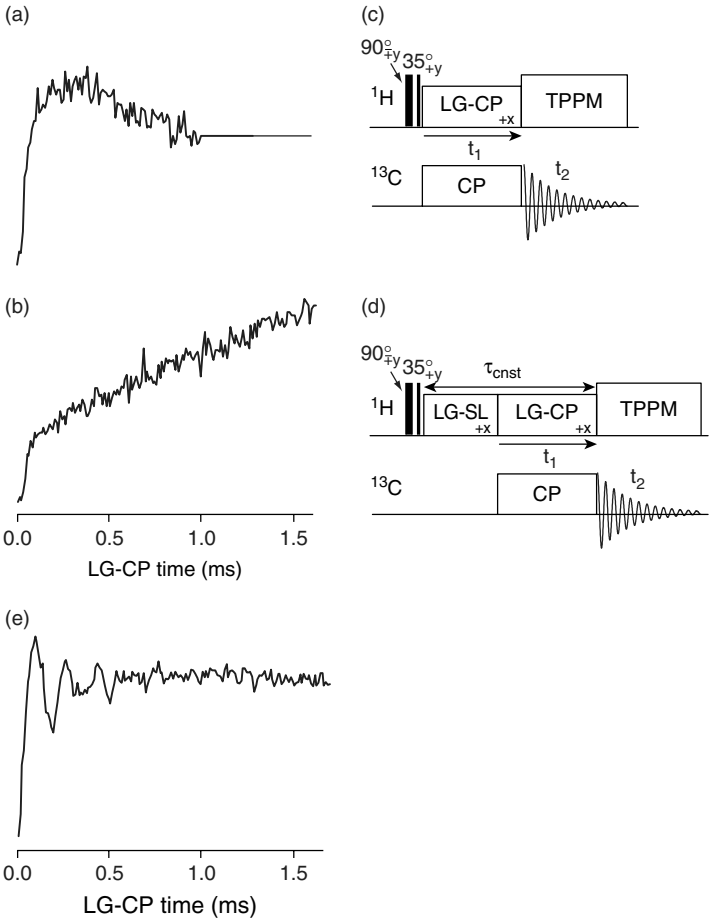

Figure 4. (a) and (b) $^{13}C-^{1}H$ LG–CP time evolution of the Val-1 Cα site of poly(Lys-25) at 30% hydration. Trace (a) exhibits clear ^{1}H $T_{1\rho}$ relaxation within 1 ms of contact time, and was acquired using the unmodified LG–CP sequence (c). This fast relaxation is removed in the time trace (b) by using the constant-time version of the LG–CP sequence, shown in (d). In this way, small couplings are manifested. For comparison, the time oscillation of Val Cα in the dry protein is shown in (e).

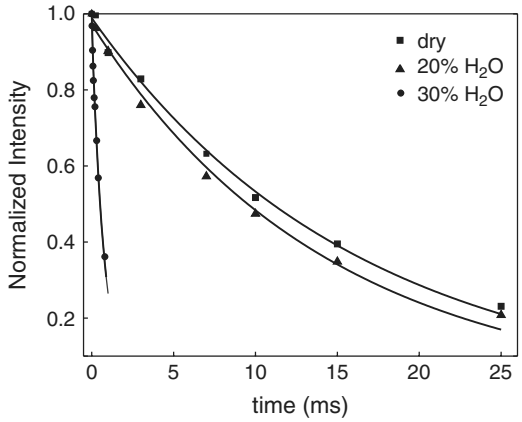

Figure 5. ^{1}H $T_{1\rho}$ relaxation curves for Val-1 Cα in dry (squares), 20% hydrated (triangles) and 30% hydrated (circles) poly(Lys-25). The ^{1}H spin lock field strength was 75 kHz. Note the similarity of the decay constants between 0 and 20% hydration and the much faster decay at 30% hydration.

as shown previously for colicin Ia channel domain.[25] We consider the ^{1}H $T_{1\rho}$ relaxation to be driven mainly by $^{13}C-^{1}H$ (δ_{CH}) and $^{1}H-^{1}H$ (δ_{HH}) dipolar couplings. Under the magic-angle spin lock, ^{1}H $T_{1\rho}$ can be written as[25]

$$\frac{1}{T_{1\rho}} = \frac{1}{10}\delta_{HH}^2[J(\omega_e) + 2J(2\omega_e) + 6J(2\omega_H) + 6J(2\omega_H)] + \frac{1}{30}\delta_{CH}^2[2J(\omega_e) + 3J(2\omega_C) + J(\omega_C - \omega_H) + 3J(\omega_H) + 6J(\omega_C + \omega_H)] \quad (1)$$

where the spectral density function $J(\omega_i)$ is given by

$$J(\omega_i) = (1 - S^2)\frac{\tau}{1 + \omega_i^2\tau^2} \quad (2)$$

where ω_e is the effective r.f. field strength of ^{1}H, ω_H and ω_C are the Larmor frequencies of ^{1}H and ^{13}C, respectively, and S is the generalized order parameter that describes the amplitude of motion. Assuming that the C–H and H–H order parameters are the same for each resolved site, then there are only two unknown parameters in Eqn (1): the correlation time τ and the order parameter S. By measuring $T_{1\rho}$ at two different spin-lock field strengths and calculating their ratios, we cancel the term $(1 - S^2)$, thus extracting the correlation time τ.

The ^{1}H $T_{1\rho}$ values of poly(Lys-25) at three hydration levels are listed in Table 3. Overall, the $T_{1\rho}$ relaxation times are

Table 3. ^{1}H $T_{1\rho}$ values and correlation times (τ) for poly(Lys-25) at three hydration levels

	Dry			20% H_2O			30% H_2O		
	$T_{1\rho}$ (ms)			$T_{1\rho}$ (ms)			$T_{1\rho}$ (ms)		
Residue	75 kHz	50 kHz	τ(μs)	75 kHz	50 kHz	τ(μs)	75 kHz	50 kHz	τ(μs)
P/V4α	15.0	9.9	1.9	13.6	9.5	1.6	0.79	0.54	1.7
V1α	16.1	10.5	2.0	14.3	10.7	1.3	0.77	0.55	1.5
Gα	16.0	10.0	2.3	14.5	11.0	1.2	0.73	0.55	1.2
Pδ	15.6	10.4	1.9	14.1	10.7	1.2	0.71	0.49	1.6
P/Vβ	14.7	10.3	1.6	13.3	10.1	1.2	0.92	0.66	1.4
Pγ	13.9	10.0	1.5	NA[a]	NA[a]	NA[a]	0.96	0.66	1.6
Vγ	14.4	9.4	2.0	NA[a]	NA[a]	NA[a]	2.7	1.8	1.9

[a] These sites are present only at natural abundance in this selectively ^{13}C labeled sample, hence the signals are too low to be observed.

relatively uniform between the backbone and the side-chains within each sample, in contrast to the more dissimilar dipolar couplings. Using the field-dependent analysis, we found the motional correlation times to be in the range 1.2–2.3 μs, and relatively insensitive to hydration. The insensitivity of motional rates to hydration, in contrast to the large coupling reductions, can be understood by the different time-scales of the two types of measurements. The $T_{1\rho}$ relaxation is driven primarily by microsecond time-scale motions, while the dipolar couplings can be reduced by any motions faster than 10^{-5} s, which can include nanosecond and picosecond motions. Indeed, nanosecond motions were previously observed in chick aortic elastin using ^{13}C T_1 relaxation measurements.[12] It was found that the hydrophobic part of the protein has an average correlation time of 65 ns for the Val carbonyl carbon.[12]

The hydration-induced motion also affected the ^{13}C spin–spin relaxation times (T_2). As shown for Gly Cα and Val Cγ sites in the dry and 20% hydrated samples (Fig. 6), ^{13}C T_2 times decrease upon hydration. In the dry protein, the ^{13}C T_2 values range from 10 ms for the mobile Val Cγ and the unprotonated carbonyl carbon to 3.4 ms for other sites. Hydration to 20% reduced the T_2 values by about 40%. This suggests that motions with rates comparable to the ^{1}H decoupling field strength have occurred to reduce the intensities.

These intrinsic ^{13}C T_2 times are much longer than the apparent T_2s estimated from the ^{13}C line widths for both the dry and the hydrated poly(Lys-25). The ^{13}C linewidths, which are 300–400 Hz for most sites except the methyl carbon, correspond to apparent T_2 values of ~0.1 ms, much shorter than the intrinsic T_2 values. Hence the ^{13}C peaks are significantly inhomogeneously broadened, indicating the existence of conformational distribution and possibly also solid-state packing effects. The apparent ^{13}C linewidths are slightly reduced at 20% hydration, despite the shortened T_2 values. Therefore, the conformational and packing distribution are mitigated by hydration, but the effect is small compared with the residual structural heterogeneity.

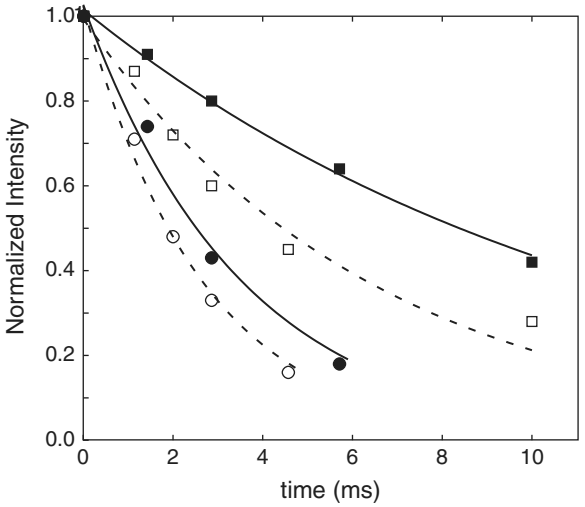

Figure 6. ^{13}C T_2 relaxation curves of Gly Cα (squares) and Val Cγ (circles) in the dry (filled symbols) and 20% hydrated (open symbols) protein.

DISCUSSION

We have examined the effect of water on the dynamics of an elastin-mimetic protein with a repeat sequence of VPGVG. This study complements a recent characterization of bovine elastin, which found that hydration induces significant mobility in the protein, evidenced by the difference in the CP and DP spectra and by ^{13}C T_1 and ^{1}H $T_{1\rho}$ relaxation times.[13] However, no quantitative motional amplitudes or time-scales were extracted from that study. The current work yields the motional amplitudes from the site-resolved dipolar couplings and motional correlation times from various relaxation times. Both the dipolar coupling measurements and CP/DP spectral series indicate unambiguously that water increases the segmental motions in the protein backbone and side-chains. Moreover, the molecular motion depends on the water content in a non-uniform manner. The protein backbone does not show much increased motion between 0 and 20% hydration but becomes drastically mobile at and above 30% hydration. This is reflected by the weaker ^{1}H–^{1}H and ^{13}C–^{1}H dipolar couplings (with order parameters of <0.1), the reduced ^{13}C CP intensities and the narrower DP linewidths. These indicate that the protein backbone undergoes near isotropic, large-amplitude motion above 30% hydration. The side-chains exhibit the same trend, but their amplitudes are larger than the backbone at each hydration

level owing to their inherent conformational flexibility. The ^{1}H $T_{1\rho}$ relaxation times exhibit a similar trend: the relaxation times decrease with increasing water non-uniformly, with the 30% hydrated protein having 20-fold shorter $T_{1\rho}$ values than the dry protein. The field dependence of $T_{1\rho}$ indicates that the motional rates remain roughly constant with hydration, at 1.2–2.3 μs. Thus, the faster $T_{1\rho}$ relaxation results primarily from the increase in the motional amplitudes, which can occur on time-scales faster than measurable by the ^{1}H $T_{1\rho}$ experiment. The clear field dependence of the ^{1}H $T_{1\rho}$ relaxation and the dramatic reduction of $T_{1\rho}$ at 30% hydration indicate that the elastin-mimetic poly(Lys-25) is highly mobile on the microsecond time-scale. The reduction of ^{13}C T_2 relaxation times by hydration also suggests micro- to millisecond time-scale motions. The abundance of slow motions in elastin provides direct experimental evidence to the model that low-frequency and large-amplitude motions in the relaxed state contribute to the entropic driving force for elasticity.[1]

The non-uniform hydration dependence of protein motion supports the hypothesis[34,35] that there are multiple types of water molecules interacting with this predominantly hydrophobic protein. The first added water molecules may be tightly bound to the protein and may participate in hydrogen bonding with the protein backbone. In this way, they may have little effect on the polypeptide chain dynamics. In fact, if every peptide bond in poly(Lys-25) is hydrogen bonded to a water molecule, then the hydration content should be about 20%, which is exactly the threshold at which we observe the onset of large-amplitude motions. Once this layer of tight structural waters is complete, additional water molecules greatly enhance the motions in the backbone and side-chains, as these water molecules are only loosely associated with the protein. The preferential suppression of the Val methyl CP signal (19 ppm) at 40% hydration indicates that these excess water molecules interact directly with both the hydrophobic side-chains and the backbone. Hence hydrophobic hydration plays a significant role in the elasticity of hydrated elastin.

At high hydration levels, the motional amplitudes of poly(Lys-25) exhibit a small degree of heterogeneity. This is manifested in the LG-CP and WISE spectra as the co-existence of a dominant mobile component and a minor rigid component. This dynamic heterogeneity may result from a combination of water–protein phase separation at the relatively high spinning speed used for the LG–CP experiment and different protein conformations that respond to hydration differently. The latter is suggested by independent distance measurements on $(VPGVG)_3$ peptides, which show two distinct conformations, a tight β-turn structure and a more open β-strand conformation (X. L. Yao and M. Hong, unpublished results).

While the molecular motion of poly(Lys-25) is significantly enhanced by water, the protein conformational distribution is largely unaffected by hydration. This is reflected by the fact that the observed ^{13}C linewidths for backbone sites do not decrease much with the addition of water. This contrasts with lysozyme, which exhibits dramatic line narrowing on addition of water, indicating a reduced conformational distribution.[36]

While poly(Lys-25) exhibits motional heterogeneity between the backbone and the side-chains, within each type of segment the motional amplitudes and rates are very similar. This differs from a leucine-zipper protein examined recently, where two relatively rigid domains co-exist with a highly mobile, water-swollen domain owing to amino acid sequence differences.[37] Poly(Lys-25) also contrasts with the hydration dynamics of spider silk, a structural protein without a pronounced sequence heterogeneity. There, the Ala residues are clearly more rigid than the other residues owing to the preferential location of Ala in crystalline regions of silk. In contrast, the $(VPGVG)_n$ polypeptide does not appear to form any phase-separated domains.

The mobility of poly(Lys-25) is far more pronounced than those of several other proteins that have been studied in the solid state under similar hydration conditions. The 30% hydrated colicin Ia channel domain in the water-soluble state shows motional amplitudes of only 0–10° for the backbone and 16–17° for the side-chains. The membrane-bound colicin Ia channel domain, which is more dynamic, also has relatively high C–H order parameters of 0.60–0.93.[25] The other important structural protein in connective tissue, collagen, exhibits small r.m.s. angles of <10° in intact and hydrated tissue samples,[9] consistent with the role of collagen in providing rigidity. In the light of these other proteins, the C–H order parameters of <0.1 at 30% hydration for poly(Lys-25) are remarkable. Thus, even moderate hydration induces extraordinary conformational flexibility in elastin. In contrast, most globular proteins respond to hydration by structural ordering rather than enhanced motion, as seen for lysozyme,[36] ubiquitin[19] and α-spectrin SH3 domain.[38] The strong hydration dynamics of elastin suggest that the protein has an open structure that allows water to induce considerable local motion. A similar dynamic response to hydration has also been observed in glycogen, a highly branched polysaccharide with a large void volume.[39]

The large-amplitude motion of elastin at moderate hydration correlates well with its functional need to provide a high-entropy relaxed state. The molecular origin of this conformational flexibility may be the hydrophobic nature of the protein: the lack of hydrogen bonds between water and the amino acid side-chains and the possible lack of hydrogen bonds between the backbone atoms could both contribute to elastin dynamics in water. Therefore, structural information for elastin at the molecular level should provide complementary insight into elastin dynamics. A structural investigation will be presented in a later paper.

Acknowledgments

The authors thank R. A. McMillan for synthesizing the protein. This work was partially supported by Iowa State University through a University Research Grant. M.H. acknowledges support by the Sloan Foundation through a Research Fellowship and the National Science Foundation for a CAREER award (MCB-0093398). V.P.C. acknowledges NASA for support (NAG8-1579).

REFERENCES

1. Urry DW. *J. Protein. Chem.* 1988; **7**: 1.
2. Debelle L, Tamburro AM. *Int. J. Biochem. Cell Biol.* 1999; **31**: 261.
3. Gary WR, Sandberg LB, Foster JA. *Nature (London)* 1973; **246**: 461.
4. Weis-Fogh T, Anderson SO. *Nature (London)* 1970; **227**: 718.
5. Gosline JM. *Biopolymers* 1978; **17**: 677.
6. Crewther WG. *Symp. on Fibrous Proteins*. Plenum Press: New York, 1968; 236.
7. Patridge SM. *Adv. Protein Chem.* 1962; **17**: 227.
8. Jelinski LW, Sullivan CE, Torchia DA. *Nature (London)* 1980; **284**: 531.
9. Sarkar SK, Sullivan CE, Torchia DA. *Biochemistry* 1985; **24**: 2348.
10. Jelinski LW, Torchia DA. *J. Mol. Biol.* 1980; **138**: 255.
11. Yang Z, Liivak O, Seidel A, LaVerde G, Zax DB, Jelinski LW. *J. Am. Chem. Soc.* 2000; **122**: 9019.
12. Fleming WW, Sullivan CE, Torchia DA. *Biopolymers* 1980; **19**: 597.
13. Perry A, Stypa MP, Tenn BK, Kumashiro KK. *Biophys. J.* 2002; **82**: 1086.
14. McMillan RA, Conticello VP. *Macromolecules* 2000; **33**: 4809.
15. Urry DW. *Methods Enzymol.* 1982; **82**: 673.
16. Urry DW. *J. Protein Chem.* 1984; **3**: 403.
17. Urry DW, Trapane TL, Prasad KU. *Biopolymers* 1985; **24**: 2345.
18. Hong M, Isailovic D, McMillan RA, Conticello VP. *Biopolymers* 2003; **70**: 158.
19. Hong M. *J. Magn. Reson.* 1999; **139**: 389.
20. Hong M, Jakes K. *J. Biomol. NMR* 1999; **14**: 71.
21. Castellani F, vanRossum B, Diehl A, Schubert M, Rehbein K, Oschkinat H. *Nature (London)* 2002; **420**: 98.
22. LeMaster DM, Cronan JE Jr. *J. Biol. Chem.* 1982; **257**: 1224.
23. Schmidt-Rohr K, Clauss J, Spiess HW. *Macromolecules* 1992; **25**: 3273.
24. Lee M, Goldburg WI. *Phys. Rev. A* 1965; **140**: 1261.
25. Huster D, Xiao L, Hong M. *Biochemistry* 2001; **40**: 7662.
26. Hong M, Yao XL, Jakes K, Huster D. *J. Phys. Chem. B* 2002; **106**: 7355.
27. Van Rossum BJ, De Groot CP, Ladizhansky V, Vega S, De Groot HJM. *J. Am. Chem. Soc.* 2000; **122**: 3465.
28. Soubias O, Reat V, Saurel O, Milon A. *J. Magn. Reson.* 2002; **158**: 143.
29. Henry ER, Szabo A. *J. Chem. Phys.* 1985; **82**: 4753.
30. Ishii Y, Terao T, Hayashi S. *J. Chem. Phys.* 1997; **107**: 2760.
31. Ladizhansky V, Vega S. *J. Chem. Phys.* 2000; **112**: 7158.
32. Palmer AG, Williams J, McDermott A. *J. Phys. Chem.* 1999; **100**: 13 293.
33. Sarkar SK, Torchia DA, Kopple KD, VanderHart DL. *J. Am. Chem. Soc.* 1984; **106**: 3328.
34. Ellis GE, Packer KJ. *Biopolymers* 1976; **15**: 813.
35. Li B, Alonso DO, Bennion BJ, Daggett V. *J. Am. Chem. Soc.* 2001; **123**: 11 991.
36. Kennedy SD, Bryant RG. *Biopolymers* 1990; **29**: 1801.
37. Kennedy SB, deAzevedo ER, Petka WA, Russell TP, Tirrell DA, Hong M. *Macromolecules* 2001; **34**: 8675.
38. Pauli J, vanRossum B, Forster H, deGroot HJM, Oschkinat H. *J. Magn. Reson.* 2000; **143**: 411.
39. Jackson CL, Bryant RG. *Biochemistry* 1989; **28**: 5024.